Radioimmunotherapy of Medullary Thyroid Cancer with Iodine-131-Labeled Anti-CEA Antibodies

Malik Juweid, Robert M. Sharkey, Thomas Behr, Lawrence C. Swayne, Thomas Herskovic, Michael Pereira, Arnold D. Rubin, Debra Hanley, Robert Dunn, Jeffry Siegel and David M. Goldenberg
Garden State Cancer Center, Center for Molecular Medicine and Immunology, Newark, New Jersey; and St. Joseph's Hospital and Medical Center, Paterson, New Jersey

This study evaluates the pharmacokinetics, dosimetry, toxicity and therapeutic potential of radiolabeled NP-4 and MN-14 anti-CEA antibodies in medullary thyroid cancer (MTC). **Methods:** Eighteen patients with advanced MTC entered exploratory clinical studies with therapeutic doses of ^{131}I-labeled NP-4 and MN-14 murine monoclonal antibodies (MAbs) reactive with carcinoembryonic antigen (CEA). Doses administered ranged from 46 mCi for ^{131}I-MN-14 IgG to 195 mCi for ^{131}I-MN-14 F(ab)$_2$ in patients negative for human anti-mouse antibodies (HAMA). **Results:** The radioconjugate blood half-life (T1/2) for the whole IgG was 42.5 ± 5.0 hr compared to 18.8 ± 4.1 hr for the bivalent fragments. Tumor doses of 17.5 ± 11.0 and 11.4 ± 6.3 cGy/mCi were estimated for ^{131}I-MN-14 IgG and F(ab)$_2$, respectively. Tumor/red marrow dose ratios exceeded 3:1 for most lesions. Red marrow doses of up to 350 cGy generally could be delivered with < grade 4 toxicity. Seven of 14 evaluable patients showed evidence of anti-tumor effects lasting up to 26 months, based on physical exam, tumor markers or computed tomography. **Conclusion:** This study demonstrates that anti-CEA MAbs may be suitable for radioimmunotherapy of metastatic or recurrent MTC.

Key Words: radioimmunotherapy; medullary thyroid cancer; carcinoembryonic antigen; monoclonal antibodies

J Nucl Med 1996; 37:905–911

Medullary thyroid cancer (MTC) confined to the thyroid gland is potentially curable by total thyroidectomy and central lymph node dissection. The prognosis of patients with unresectable disease or distant metastases, however, is poor; less than 30% survive 10 yr (*1–3*). These patients are left with few therapeutic choices (*4,5*). Chemotherapy has been of little value and radiation therapy may only be used to control local disease (*5,6*). Thus, new therapeutic modalities are needed in this precarious clinical setting.

MTCs express and release carcinoembryonic antigen (CEA) (*7–10*), and plasma CEA levels are used, in addition to calcitonin, to monitor disease in these patients. Moreover, pronounced CEA elevations appear to be prognostically more reliable in patients with metastatic disease, often associated with a more aggressive tumor (*11*). Therefore, it seemed logical to utilize radiolabeled anti-CEA monoclonal antibodies (MAbs) for the targeting and potential treatment of residual (recurrent) or metastatic MTC. In this respect, sites of disease could be targeted and treated in those patients where a more aggressive intervention may be indicated.

We have previously shown excellent targeting of MTC with radiolabeled anti-CEA antibodies (*12*). In the present study, we report the pharmacokinetics and dosimetry results in patients who received ^{131}I-labeled anti-CEA antibodies. In addition, we describe the initial therapeutic results in 14 patients evaluated for anti-tumor responses.

Received Apr. 27, 1995; revision accepted Aug. 22, 1995.
For correspondence or reprints contact: David M. Goldenberg, MD, Garden State Cancer Center, Center for Molecular Medicine and Immunology, 1 Bruce St., Newark, NJ 07103.

METHODS

Patients

Patients with histologically-proven MTC, both familial and sporadic, were eligible. Most patients had established disease clinically or radiologically at the time of their presentation. However, four patients with a prior history of MTC were referred because of elevated plasma calcitonin or CEA, but without radiological evidence of disease. These patients were only eligible for treatment in this study if a pre-therapy antibody imaging study unequivocally revealed tumor. Radiologic correlative studies, such as CT, were performed within 4 wk prior to antibody imaging or treatment, with follow-up CT studies performed at a minimum of 1 and 3 mo. Circulating calcitonin and CEA were measured on the day of treatment and in 1–3-mo intervals for 1 yr or more thereafter. For entry into the therapy studies, patients were at least 4 wk beyond any major surgery, radiation or chemotherapy, and must have recovered from any prior treatment-induced toxicity. The patients had a performance status of ≥70 on the Karnofsky scale (ECOG 0-2) and a minimal life expectancy of 3 mo, no severe anorexia, nausea or vomiting, normal hepatic and renal function, WBC ≥3,000/mm^3 or a granulocyte count ≥1500/mm^3 and a platelet count ≥100,000. Subjects were excluded from treatment if they were pregnant, or had extensive irradiation to more than 25% of their red marrow within 1 yr of treatment. A baseline blood anti-mouse antibody (HAMA) titer was determined in all patients, with follow-up at 1, 2, 4, 8 and 12 wk. HAMA was monitored in most patients by the ImmuSTRIP™ HAMA IgG assay (Immunomedics, Inc., Morris Plains, NJ), but in two patients, HAMA was monitored by a HAMA titer assay (*17*). CEA was determined in-house by an immunoassay that eliminates interference with HAMA (*17*). Other assays were performed by registered clinical laboratories. All patients signed an informed consent. All protocols were approved by the governing Institutional Review Board.

Antibody Preparation and Testing

The murine IgG$_1$ NP-4 (Immu-4) and MN-14 (Immu-14) MAbs are directed against the Class III, CEA-specific epitope according to the classification of Primus et al. (*13*). They were selected because of their excellent tumor targeting properties, and lack of binding to cross-reactive antigens such as NCA or to normal tissues (*14–16*). The F(ab')$_2$ fragment of NP-4 was prepared by pepsin digestion, while the F(ab)$_2$ fragment of MN-14 was prepared by papain digestion. Removal of undigested IgG was by protein-A followed by repeated ultrafiltration. Most patients received MN-14 IgG or F(ab)$_2$, a second-generation anti-CEA MAb that was found to have a tenfold higher affinity ($1 \times 10^9 M^{-1}$) than NP-4, and superior tumor targeting in a human colon tumor xenograft model (*14*).

TABLE 1
Antibody Infusions and Sites of Disease

Patient no.	No. of injections	Sex	Age (yr)	Antibody infusion*	Sites of disease†
600	1	M	18	10.8 mCi (0.7 mg) ^{131}I-NP-4 IgG	Bone, liver, cervical lymph nodes
	2			129.0 mCi (8 mg) ^{131}I-NP-4 IgG (7)	
	3			130.0 mCi (7 mg) ^{131}I-NP-4 IgG (29)‡	
	4			268.0 mCi (20 mg) ^{131}I-NP-4 IgG (36)‡	
	5			238.0 mCi (19 mg) ^{131}I-NP-4 IgG (42)‡	
718	1	M	23	260.0 mCi (19 mg) ^{131}I-NP-4 IgG‡	Liver, hilar and peri-aortic lymph nodes
	2			246.0 mCi (20.7 mg) ^{131}I-NP-4 IgG (16)‡	
1431	1	F	59	66.6 mCi (4.5 mg) ^{131}I-NP-4 IgG	Bone, cervical lymph nodes, liver
1318	1	M	40	111 mCi (13 mg) ^{131}I-NP-4 F(ab')$_2$	Cervical lymph nodes
	2			244 mCi (25 mg) ^{131}I-NP-4 F(ab')$_2$ (35)‡	
1247	1	F	72	77.2 mCi (5.9 mg) ^{131}I-MN-14 IgG	Thyroid, bone, liver
1261	1	F	41	73.4 mCi (5.9 mg) ^{131}I-MN-14 IgG	Cervical lymph nodes, bone
1465	1	F	20	8.1 mCi (0.6 mg) ^{131}I-MN-14 IgG	Cervical, mediastinal, and peri-aortic lymph nodes, lungs, liver, bone
	2			45.8 mCi (10.0 mg) ^{131}I-MN-14 IgG (1)	
1485	1	F	46	8.7 mCi (0.6 mg) ^{131}I-MN-14 IgG	Liver
	2			56.9 mCi (5.1 mg) ^{131}I-MN-14 IgG (1)	
1332	1	M	61	77.2 mCi (9.5 mg) ^{131}I-MN-14 F(ab)$_2$	Mediastinal lymph nodes, lung, liver
1346	1	M	65	98.0 mCi (8.0 mg) ^{131}I-MN-14 F(ab)$_2$	Bone, liver, peri-aortic lymph nodes
1361	1	M	44	138 mCi (12 mg) ^{131}I-MN-14 F(ab)$_2$	Cervical and mediastinal lymph nodes, lungs
	2			238 mCi (18 mg) ^{131}I-MN-14 F(ab)$_2$ (16)‡	
1480	1	M	65	8.4 mCi (0.7 mg) ^{131}I-MN-14 F(ab)$_2$	Mediastinal lymph nodes
	2			147.3 mCi (14.8 mg) ^{131}I-MN-14 F(ab)$_2$ (1)	
1520	1	M	56	8.0 mCi (0.6 mg) ^{131}I-MN-14 F(ab)$_2$	Cervical lymph nodes, lungs, liver
	2			163.8 mCi (12.1 mg) ^{131}I-MN-14 F(ab)$_2$ (1)	
1527	1	M	53	8.1 mCi (10.0 mg) ^{131}I-MN-14 F(ab)$_2$	Mediastinal lymph nodes, liver
	2			148.0 mCi (10.7 mg) ^{131}I-MN-14 F(ab)$_2$ (1)	
1547	1	M	15	7.6 mCi (0.8 mg) ^{131}I-MN-14 F(ab)$_2$	Cervical, mediastinal, peri-aortic and iliac lymph nodes, lungs, liver
	2			89.6 mCi (9.6 mg) ^{131}I-MN-14 F(ab)$_2$ (1)	
1556	1	M	30	8.3 mCi (0.8 mg) ^{131}I-MN-14 F(ab)$_2$	Cervical and mediastinal lymph nodes
	2			100.3 mCi (7.9 mg) ^{131}I-MN-14 F(ab)$_2$ (1)	
1578	1	M	76	8.1 mCi (0.6 mg) ^{131}I-MN-14 F(ab)$_2$	Mediastinal lymph nodes
	2			121.0 mCi (9.3 mg) ^{131}I-MN-14 F(ab)$_2$ (1)	

*Number in parentheses is the number of weeks following the first injection of this study.
†Site of disease disclosed by CT, MRI, bone scan, radiography, ultrasound, surgery or by the antibody scan.
‡Patient had HAMA at the time of infusion.

Radiolabeling and Quality Assurance

NP-4 and MN-14 IgG or fragments were labeled with ^{131}INa by the iodogen method to a specific activity of 12–16 mCi/mg as described previously (*15*). Every labeled product was analyzed by size-exclusion HPLC and instant thin-layer chromatography to determine aggregation and unbound radioiodine, and by affinity chromatography for immunoreactivity. More than 70% binding to a CEA immunoabsorbent was found for the radiolabeled antibody. Less than 2% unbound isotope and <7% aggregation were demonstrated by HPLC for all agents. HPLC analysis of plasma indicated that radiolabeled NP-4 and MN-14 bivalent fragments were stable in vivo with less than 10% or 15% Fab at 1 and 24 hr, respectively.

Antibody Infusions

Table 1 lists the patients who received therapeutic infusions of radiolabeled anti-CEA antibodies.

Patients with MTC were entered into either one of two separate Phase I trials that were active at the time of their admission. In the first Phase I trial, the radioactive dose of MN-14 or NP-4 administered was based on the body surface area starting at 30 mCi/m^2 for IgG and 45 mCi/m^2 for F(ab)$_2$ and escalating in 10 or 15 mCi/m^2 increments for the IgG or F(ab)$_2$, respectively. MTC patients were entered with other patients with CEA-producing tumors and therefore received the dose level allowed at the time of study entry. Sixteen of the 18 patients included in this study were treated under this protocol. Subsequently, an MTC-specific Phase I therapy trial with ^{131}I-MN-14 F(ab)$_2$ was developed. Two patients were treated to date under this protocol at a dose of 70 mCi/m^2.

Overall, a total of 18 MTC patients (12 men, 6 women; aged 15–72 yr) received therapeutic doses of radiolabeled anti-CEA antibodies. One patient (718) received a therapeutic dose of NP-3 MAb before receiving NP-4 and was therefore excluded from the final evaluation. Of the 17 assessable patients, two received ^{131}I-NP-4 IgG, one received ^{131}I-NP-4 F(ab')$_2$, four received ^{131}I-MN-14 IgG and ten received ^{131}I-MN-14 F(ab)$_2$. Eight of the 17 patients received a diagnostic study with the same anti-CEA MAb (8 mCi, 1 mg) 1 wk before therapeutic infusion, and four patients received more than one therapy injection. In patients without HAMA, treatment doses of ^{131}I-MAb ranged from 46 mCi (4.1 mg) of ^{131}I-MN-14 IgG to 195 mCi (17.5 mg) of ^{131}I-MN-14 F(ab)$_2$. Three patients who developed HAMA after their first treatment received higher radioactive doses of 239 mCi of ^{131}I-MN-14 F(ab)$_2$, 244 mCi of ^{131}I-NP-4 F(ab')$_2$ and 268 mCi of ^{131}I-NP-4 IgG, respectively. All injections were given intravenously, proceeding slowly over the first 5 min, and then at a more rapid rate to complete the infusion within 15–30 min. All patients receiving radioiodinated MAbs were premedicated with Lugol's solution (5 drops orally, three times/day) and potassium perchlorate (200 mg orally, two times/day) to decrease thyroid and gastric uptake of radioiodine. Although most patients had a total thyroid-

ectomy, Lugol's was given to minimize radioiodine uptake in any residual thyroid tissue, which could potentially be confused with tumor.

Pharmacokinetic Analysis

Blood clearance rates were determined by counting samples of whole blood at various time points after the end of the infusion. Three to five blood samples were taken over the first 24 hr, and then daily sampling was performed over the next 2–6 days. Estimates of the slopes of the distribution (alpha) and elimination (beta) phases, and their respective intercepts, were then used in a nonlinear, least squares, curve-fitting program to generate both monophasic and biphasic clearance curves. If the biphasic result significantly improved the sum of the squares, then it was selected as the best fit; otherwise, the monophasic curve was used to define the blood clearance. The radioconjugate blood T1/2 was defined as the time required to clear 50% of the initial radioactivity from the blood.

Imaging

Planar imaging (500K counts per view) consisting of anterior and posterior scans of the head, chest, abdomen and pelvis were obtained using cameras equipped with a high-energy collimator. Images were taken at 4 hr and then daily for 1 wk postinfusion of a diagnostic dose of the antibodies using a 128 × 128 matrix. Post-therapy imaging was initiated when the level of activity fell below 5 mR/h at 1 m, usually 3–5 days postantibody infusion. SPECT studies (64 × 64 matrix size) of the chest, abdomen and pelvis were obtained on at least one occasion 24 hr or later postinfusion. SPECT was used to better identify the tumor site by improved contrast resolution and to calculate the tumor volumes for the dosimetric studies.

Dosimetry

An activity quantification technique for the gamma camera based on the build-up factor methodology, as described elsewhere (*18*), was used. Anterior and posterior planar images of the chest, abdomen and pelvis were obtained for at least three imaging sessions (usually 24, 48 and 72 hr). Tumor volumes were measured by means of our previously validated SPECT volume program (*19*). This procedure was also used to estimate the volume of organs that appeared abnormal in size. Otherwise, the standard human weights given by Medical Internal Radiation Dose (MIRD) (*20*) were used. The organ and tumor time-activity data were then fitted to either an exponential function by a nonlinear, least squares curve-fitting routine, or by a trapezoidal modeling method, and then integrated to obtain the cumulated activity. The cumulated activity in the red marrow was calculated from the blood by assuming an equal activity concentration at equilibrium between blood and red marrow as suggested by Bigler et al. (*21*). This assumption was used to obtain the most conservative estimate of the red marrow dose. The blood activity concentration was then multiplied by 1500, the weight in grams of the marrow in an average adult. The mean dose in cGy (rad) to the various target organs, with the exception of the tumors, was then obtained according to the MIRD schema with correction for the remainder of the body activity (*20,22*). The mean dose in cGy to the tumors was obtained by the previously reported method (*18*).

Toxicity and Tumor Response

Toxicity was graded according to the Radiation Therapy Oncology Group (RTOG) criteria. All patients given therapeutic doses of ^{131}I-MAbs were followed for toxicity by monitoring complete peripheral blood cell counts weekly. Renal and hepatic function were assayed 7 and 28 days post-therapy. Tumor responses were assessed at 1 to 3 mo after treatment and every 3 mo thereafter, up to 1 yr. If disease progression occurred after 3 mo, no further follow-up was attempted. In addition to physical exams, chest radiograph, CT and MRI were used to assess therapeutic response. Both tumor markers in the blood (CEA and calcitonin) were assessed at 1–3 mo, up to 1 yr post-therapy. Reduction in tumor markers that was >25% for at least 1 mo was considered as indicative of an anti-tumor effect. A complete remission was defined as the complete disappearance of all detectable disease for a minimum of 4 wk, a partial response as a reduction of at least 50% in the sum of the products of the longest perpendicular diameters of all measurable lesions for a minimum of 4 wk, and disease progression as an increase of at least 25% in the diameter or the appearance of new lesions. Minor responses were considered when the reduction in disease was between 25% and 50%.

RESULTS

Pharmacokinetics

A review of the pharmacokinetic behavior of the labeled antibody in the blood showed considerable variability in the clearance rates. These differences were due to HAMA and, to a variable degree, to differences in the level of circulating CEA. Thus, to compare the pharmacokinetic behavior of whole IgG and fragments, only injections in patients who were negative for HAMA and with <30% complexation with circulating antigen, as detected by HPLC, were included. In this group of patients, variability in the plasma clearance within each form of immunoglobulin was minimal. For example, in seven patients given the whole IgG (nine injections), the average T1/2 in the blood was 42.5 ± 5.0 hr, whereas in 11 patients (18 injections) given the antibody fragment, the clearance rate 18.8 ± 4.1 hr. These data suggest that the fragment is cleared at a rate twofold faster than the IgG form.

HAMA accelerated the rate of antibody clearance from the blood by 5- to 10-fold for both the IgG and fragment. In patients with high levels of antibody complexation with circulating CEA (i.e., >30%), altered clearance and biodistribution were observed. However, this effect was variable, resulting in a more rapid clearance in two patients, but a slower clearance in another two patients. These four patients were HAMA-negative by our assay. Because of the relatively small number of patients, it was not possible to determine the underlying cause of this variability. The clearance of the antibody-CEA complexes, however, may be mediated by CEA receptors in the liver, and their clearance may vary depending on different subtypes of CEA in different tumors. In support of this hypothesis, increased liver uptake was noted in one HAMA-negative patient who had an elevated CEA of 124 ng/ml and 50% complexation. This patient was given 0.5 mg of ^{131}I-MN-14 IgG and cleared the antibody from the blood with a T1/2 of only 14 hr.

There was good correlation between the CEA level in plasma and antibody complexation. Complexation with CEA, however, was also dependent on the protein dose given. Increasing the protein dose reduced complexation and resulted in further "normalization" of antibody clearance. This was demonstrated in two patients with high complexation (i.e., >30%), who received low (~1 mg) and high (10 mg) protein doses with their labeled antibody infusions given 1 wk apart. The influence of protein dose on the antibody pharmacokinetics in MTC patients will be reported in detail elsewhere (Juweid et al., unpublished data).

Targeting

Tumor targeting was seen in all 17 assessable patients who received therapeutic doses of ^{131}I-labeled anti-CEA MAbs. Overall, 122 of 131 (93%) confirmed lesions were revealed.

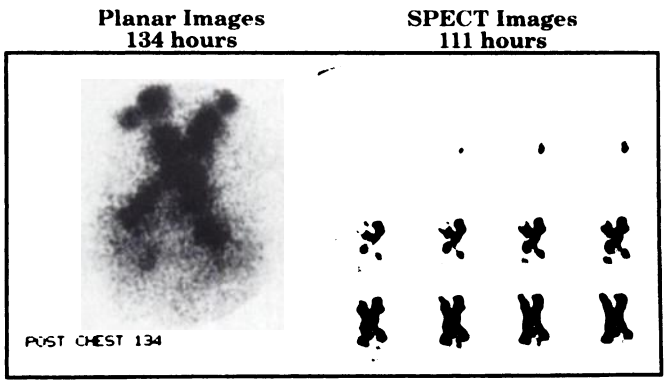

FIGURE 1. Planar (left side) and SPECT coronal images (right side; the frames proceed from left to right and posterior to anterior) of Patient 1361 obtained 6 days after the first RAIT with 138.4 mCi ^{131}I-MN-14 F(ab)$_2$. The images demonstrate the cervical and mediastinal adenopathy and multiple lesions in both lungs. This patient achieved a 45% regression of cervical adenopathy by physical exam after RAIT.

Figure 1 shows an example of tumor targeting in one patient with metastatic MTC. The images were obtained 6 days after the first RAIT with 138.4 mCi of ^{131}I-MN-14 F(ab)$_2$ and demonstrate cervical and mediastinal adenopathy in addition to multiple lesions in both lungs.

Tumor and Organ Dosimetry

Table 2 gives the average tumor, total body and normal organ absorbed dose estimates obtained with the ^{131}I-labeled anti-CEA MAbs. Doses to organs that were diffusely infiltrated with tumors, such as lungs or liver, were not included in the calculation. The absorbed radiation doses (in cGy/mCi) to red marrow, lungs and liver were almost twofold lower with the F(ab)$_2$ of MN-14 than with the IgG form ($p < 0.05$). The kidney doses, however, were similar with both agents.

Tumor weights ranged from 10 to 1275 g (n = 38). The biological half-life of the MAbs in the tumors ranged from 2 to 25 days. However, 18 of 38 lesions (47%) had half-lives >3 days. The mean tumor doses for MN-14 IgG and F(ab)$_2$ were 17.5 ± 11.0 and 11.4 ± 6.3 cGy/mCi, respectively. The average tumor-to-nontumor absorbed dose ratios obtained with MN-14 IgG were 18.1 ± 13.2, 4.6 ± 3.6, 3.5 ± 1.8, 3.0 ± 1.4 and 3.7 ± 2.3 for total body, red marrow, lung, liver and kidneys, respectively. The average tumor-to-nontumor ratios obtained with MN-14 F(ab)$_2$ were 17.1 ± 10.8, 5.8 ± 3.5, 6.4 ± 4.4, 7.5 ± 5.3 and 3.9 ± 2.7 for total body, red marrow, lung, liver and kidneys, respectively. Due to the considerable interpatient variability in tumor size, and possibly antigen content or tumor vascularization, resulting in a large standard deviation within each group, no statistically significant differences were found in the mean biological half-lives, tumor doses or tumor-to-nontumor ratios between the IgG or F(ab)$_2$ forms of MN-14, although there was a trend toward higher tumor to red marrow, lung and liver ratios with the F(ab)$_2$ form compared to IgG.

Initial Therapeutic Findings

Of the 17 patients included in this study, three patients (1465, 1332 and 1485) were not assessable due to insufficient follow-up data, leaving 14 patients who could be evaluated for tumor response. No major responses were observed; but moderate anti-tumor effects were seen in 7 of the 14 assessable subjects who received single or multiple antibody treatments (Table 3). Four patients showed some reduction in tumor size seen on physical exam or CT. As illustrated in Figure 2, imaging after the initial 48.4 mCi ^{131}I-MN-14 F(ab)$_2$ revealed all lesions with pronounced uptake in the liver metastasis. Two months later, a second injection of 195 mCi ^{131}I-MN-14 F(ab)$_2$ was given. The antibody imaging study performed after this injection continued to show uptake in both lungs, but both the size and uptake of the liver lesion had slightly decreased. A chest CT scan obtained 6 wk after this second injection demonstrated a decrease in the left malignant pleural effusion seen previously. The patient received another 145 mCi ^{131}I-MN-14 F(ab)$_2$ 3 mo after the second treatment. At this time, the MAb scan showed a decrease in measured volume and intensity of the liver lesion. The uptake in the left lung remained unchanged, possibly due to the persistent pleural effusion. CEA levels also gradually dropped from 306 ng/ml on the day of the first treatment to 121 ng/ml 1 mo after the third treatment (60% decrease). A chest CT scan performed 4 mo after the third treatment showed pleural-based densities and could not distinguish between metastases or fibrosis. However, an abdominal CT without contrast was not performed after the treatments, and the CT scan made with intravenous contrast medium failed, as it did initially, to demonstrate any liver metastases. Unfortunately, the massive spread of disease in both lungs and the advanced disease stage were limiting, and the patient eventually progressed and died of her cancer 1 yr after the last RAIT.

Toxicity

No adverse experiences were observed with any of the injections, including patients with HAMA. Table 4 lists the myelotoxicity in 16 evaluable patients who received various doses of the radiolabeled MAbs. In addition to the radioactive dose administered, the absorbed red marrow dose was calculated. Toxicity, particularly of white blood cells or platelets, occurred from 3 to 4 wk after treatment. Most patients, however, recovered fully within 6 wk, with the exception of Patient 1329, who needed 7 mo for full recovery after the third treatment. This patient had a cumulative radiation dose to the red marrow of 900 cGy over 5 mo. When grade 3 or 4 toxicity developed, as was the case in 6 of 20 RAIT courses (five patients), the duration of grade 3 toxicity was <15 days, and grade 4 toxicity <5 days, except in Patient 1329 who had grade

TABLE 2
Tumor and Organ Dosimetry (expressed as cGy/mCi)

Antibody	Tumor	Total Body	Red Marrow	Lung	Liver	Kidney
MN-14 IgG	17.5 ± 11.0* (n = 9)	1.0 ± 0.2 (n = 5)	3.8 ± 0.7 (n = 5)	4.3 ± 1.8 (n = 4)	4.4 ± 2.0 (n = 5)	5.1 ± 1.5 (n = 3)
MN-14 F(ab)$_2$	11.3 ± 6.3 (n = 25)	0.7 ± 0.2 (n = 10)	2.1 ± 1.2 (n = 10)	2.4 ± 0.6 (n = 6)	1.9 ± 0.9 (n = 9)	4.2 ± 1.5 (n = 10)
NP-4 IgG	10.0 ± 1.5 (n = 3)	0.7	2.9	3.5	2.3	3.6
NP-4 F(ab')$_2$	4.2	0.5	1.3	1.6	1.1	4.3

*Mean ± s.d.

TABLE 3
Therapeutic Results in Assessable Patients

Patient no.	Antibody	mCi Injected	cGy Dose to tumor	Anti-Tumor effects (duration)
1329	MN-14 $F(ab)_2$	48	312-1263	40% decrease in size of liver metastases after second RAIT; 60% decrease in plasma CEA over 6 mo.
	MN-14 $F(ab)_2$	195	1260-3127	
	MN-14 $F(ab)_2$	145	ND	
1318	NP4 $F(ab')_2$	111	471	Stable (1 mo)
	NP4 $F(ab')_2$	244*	ND	25% reduction in left cervical and stable right cervical adenopathy (5 mo); Stable CEA and calcitonin (11 mo).
1361	MN-14 $F(ab)_2$	138	787	45% reduction in left cervical and stable mediastinal adenopathy (5.5 mo); 45% decrease in CEA and 35% decrease in calcitonin.
	MN-14 $F(ab)_2$	239*	ND	
1346	MN-14 $F(ab)_2$	98	1000-1264	Minor reduction (<50%) in retrocrural adenopathy (duration ND).
1431	NP-4 IgG	67	556-686	Stable (2.5 mo)
1247	MN-14 IgG	77	1170-1399	Stable (5 mo)
600	MN-14 IgG	129*	ND	Stable (10 mo)
		130*	ND	
		268†	ND	
		238†	ND	
1261	MN-14 IgG	73	ND	40% drop in calcitonin (26+ mo).
1520	MN-14 $F(ab)_2$	164	1691-3990	Progression
1527	MN-14 $F(ab)_2$	148	2013-3138	Stable (6 mo)
1547	MN-14 $F(ab)_2$	90	63-1372	Progression
1556	MN-14 $F(ab)_2$	100	ND	40% decrease in calcitonin (2 mo). Stable CEA (6+ mo).
1480	MN-14 $F(ab)_2$	147	1149	Progression
1578	MN-14 $F(ab)_2$	121	1355	35% decrease in calcitonin (1 mo). 35% decrease in CEA (2 mo).

*Low levels of HAMA at the time of treatment (< 500 ng/ml).
†High levels of HAMA at the time of treatment (> 4000 ng/ml).
ND = not determined.

4 leukopenia for 12 days after the second treatment and grade 4 thrombocytopenia for 8 wk after the third treatment.

Red marrow doses that were below 350 cGy resulted in ≤grade 3 myelotoxicity, except in one patient who had a prior treatment with interferon 6 wk before radioimmunotherapy with 46 mCi ^{131}I-MN-14 IgG and had bone marrow involvement by MRI. This patient then developed a grade 4 thrombocytopenia. Grade 4 myelotoxicity occurred at a red marrow dose of 379 cGy in one patient who received a single dose of radioimmunotherapy. This patient demonstrated bone uptake by antibody imaging, which was interpreted as bony metastases. A bone scanning or MRI was not performed to confirm this finding. The other patient who developed a grade 4 toxicity at a red marrow dose of 441 cGy had previously received a red marrow dose of 97 cGy from his first therapy 2 mo earlier (total dose 538 cGy).

HAMA Induction

HAMA was monitored in all patients given the IgG, $F(ab')_2$ or $F(ab)_2$ fragments. One patient entering this program had pre-existing HAMA levels due to prior injections of murine MAb. One other patient had prior infusions of two diagnostic murine antibody studies given 6 wk apart without developing HAMA. He was, however, considered "presensitized" for HAMA development in the following infusions. This patient developed a low level of HAMA after his therapeutic infusion of 129 mCi ^{131}I-NP-4 IgG. Sixteen patients were therefore assessable for HAMA. All of the 5 patients given therapeutic doses of the IgG form developed HAMA, but only 5 of 11 patients given the bivalent fragments did so. Most notable was Patient 1329 who was given three injections of MN-14 $F(ab)_2$ and failed to develop HAMA. The protein doses given were 4.1, 17.5 and 13.1 mg, respectively.

DISCUSSION

Successful radioimmunotherapy depends on effective targeting of all tumor sites and the delivery of high tumor radiation doses, compared to normal tissues. Our targeting results in patients who received therapeutic doses of ^{131}I-labeled anti-CEA antibodies NP-4 and MN-14 indicate that this condition may be achieved in MTC. One hundred and twenty-two of 131 confirmed lesions (93%) were targeted in the 17 patients evaluated. Targeting of MTC with radiolabeled MAbs against CEA has been reported before by other investigators (*23–27*). Therapy, however, was not pursued in these studies.

The pharmacokinetic studies showed that the bivalent fragment is cleared from blood at a rate twofold faster than the IgG form. This difference cannot be due to instability of the bivalent fragments, since HPLC performed at 1 and 24 hr showed <15% Fab′ in all patients. As expected, the faster blood clearance of MN-14-$F(ab)_2$ resulted in almost twofold lower red marrow, liver and lung radiation absorbed doses compared to the IgG form ($p < 0.05$). We have also demonstrated an effect of the protein dose on antibody clearance in MTC patients with elevated plasma CEA, as we previously described for a wide range of CEA-producing tumors (*28*). The influence of protein dose on the pharmacokinetics of radiolabeled antibodies was previously reported by Murray et al. in the non-circulating antigen system of melanoma patients (*29*). Halpern et al. (*30*) and Patt et al. (*31*) have also described this phenomenon in patients with circulating CEA. Thus, if the intent is to use the diagnostic study to predict the pharmacokinetics and dosimetry

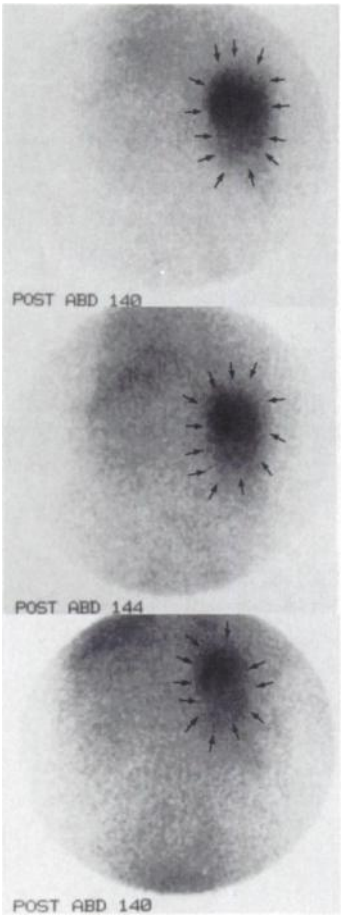

FIGURE 2. Planar images of the posterior abdomen in Patient 1329 obtained 6 days after the first (top), second (middle) and third (bottom) RAIT injection. The metastasis in the posterior right liver lobe becomes substantially smaller (40% by quantitative SPECT measurement) 3 mo after a second RAIT with 195 mCi ^{131}I-MN-14 F(ab)$_2$ (bottom image). Also note that the tumor-to-nontumor ratio is lower in the bottom image.

for a therapy infusion, the protein dose for each injection should be matched, especially in patients with high plasma CEA.

The tumor red marrow dose ratios exceeded 3:1 for most lesions (89%). The mean tumor-to-normal organs absorbed dose ratios were 3:1 or higher for both IgG and bivalent fragments. These initial studies used two different anti-CEA MAbs, with both whole IgG and bivalent fragments tested. Based on the initial results, it appears that the F(ab)$_2$ form of MN-14 may be the most suitable agent for RAIT, considering its lower immunogenicity and the trend toward higher tumor-to-red marrow, lung and liver dose ratios and similar tumor-to-kidney ratios with F(ab)$_2$ compared to the IgG. This trend was statistically confirmed in a larger group of patients with CEA-producing tumors, including medullary thyroid (Juweid et al., unpublished observations). Thus, studies are underway to determine the MTD of MN-14 F(ab)$_2$ as the agent of choice for the treatment of MTC.

Despite the fact that most patients included in this study were in a very advanced disease stage, had distant metastases to several organs and a large tumor burden, anti-tumor effects were observed. The results are particularly encouraging, since, in this study, the maximum tolerated dose has not been given to all patients. In fact, the toxicity data indicate that 11 of 16 patients evaluable for toxicity had ≤grade 2 toxicity.

In Patient 1329, who received multiple treatments with ^{131}I-MN-14 F(ab)$_2$, a 40% reduction in the size of the liver metastasis according to antibody imaging with a concordant drop in the plasma CEA level was seen. The lack of major responses indicates that a more aggressive therapeutic regimen combined with autologous red marrow or peripheral stem cell support may have been necessary in this patient. Interestingly,

TABLE 4
Myelotoxicity in MTC Patients Treated with Nonmyloablative Doses of Iodine-131-Anti-CEA MAbs

Patient no.	MAb	mCi	Radiation dose to red marrow (cGy)	Myelotoxicity grade	TTR
600	NP4-IgG	129	334	2(WBC)	33 d
1431	NP4-IgG	67	200	1(WBC)	ND
1318	NP4-F(ab')$_2$	111	147	0	—
	NP4-F(ab')$_2$	244	194	1(WBC)	7 d
1261	MN-14 IgG	73	379	4(Plat), 3(WBC), 2(RBC)	47 d
1247	MN-14 IgG	77	319	3(WBC & Plat)	41 d
1465	MN-14 IgG	46	152	4(Plat), 3(WBC), 2(RBC)	ND
1485	MN-14 IgG	57	229	0	—
1332	MN-14 F(ab)$_2$	77	97	1(RBC)	ND
1329	MN-14 F(ab)$_2$	48	97	1(WBC)	ND
	MN-14 F(ab)$_2$	195	441	4(WBC & Plat), 1(RBC)	17 d
	MN-14 F(ab)$_2$	145	365	4(Plat), 3(WBC), 1(RBC)	210 d
1346	MN-14 F(ab)$_2$	98	365	2(Plat & WBC)	15 d
1361	MN-14 F(ab)$_2$	138	170	1(WBC)	40 d
	MN-14 F(ab)$_2$	239	35	2(WBC)	8 d
1480	MN-14 F(ab)$_2$	147	250	1(WBC)	ND
1520	MN-14 F(ab)$_2$	164	349	1(WBC)	10 d
1527	MN-14 F(ab)$_2$	148	261	3(WBC), 2(Plat), 1(RBC)	21 d
1556	MN-14 F(ab)$_2$	100	221	0	—
1578	MN-14 F(ab)$_2$	121	250	1(WBC), 1(Plat)	ND

WBC = white blood cells; PLAT = platelets; RBC = red blood cells; TTR = time to recovery from the nadir of the most severe myelotoxicity; ND = not determined.

however, some anti-tumor effects, even though limited, were observed in two of our patients given relatively low radiation doses of only 471 and 787 cGy, respectively. Both patients had extensive lymphadenopathy. An explanation of this finding may be related to microscopic heterogeneity of the radiation dose within the tumor mass. The radiation dose in these lesions is calculated based on the assumption of a uniform distribution of radioactivity in a mass of uniform tumor density. The microdistribution within the mass is not seen on the antibody scan because of the limited spatial resolution of the gamma camera with ^{131}I. Such microheterogeneity is also difficult to appreciate using CT or ultrasound. This method of calculation may therefore largely underestimate the radiation dose of small tumor regions targeted. Thus, it is our belief that the observed anti-tumor effects in these patients are related to radiation doses that are higher than those calculated, and not to any radiosensitivity of MTC. The induction of apoptosis, however, may also represent another explanation for the shrinkage of certain lesions with low dose rate radiation.

CONCLUSION

Several strategies may be suitable to improve the effectiveness of radioimmunotherapy in MTC. These include the combination with other modalities such as radiotherapy or radiosensitizing agents, autologous red marrow or peripheral stem cell support and its use in patients with minimal residual disease.

Our results in patients with advanced and metastatic disease are encouraging and suggest that MTC may be a suitable target for radioimmunotherapy. Further studies are therefore warranted.

ACKNOWLEDGMENTS

We thank M. Przybylowski, D. Varga and L. Ince for preparations and quality assurance of the labeled antibody, S. Rose and S. Murthy for radiation safety assistance, R. Vagg for data management, D. Dunlop for imaging and dosimetry assistance, I. Magill and B. Magrys for assistance in immunoassays and processing pharmacokinetic data, V. Reddick for patient follow-up and S. DeVivo for nursing services. We also thank Dr. T. Kamal, University of Alabama, Tuscaloosa, AL, Dr. P. Savage, Wake Forest University Medical School, Winston-Salem, NC, and Dr. J. Gargiulo, Capitol District Radiation Oncology Group, Latham, NY, for their help in the evaluation of our common patients.

Supported in part by Outstanding Investigator grant CA39841 (Dr. Goldenberg), CA 66906-01 (Dr. Juweid) from the National Cancer Institute, National Institutes of Health, Bethesda, MD, and FD-R-001190-01 from the U.S. Food and Drug Administration (Dr. Juweid).

REFERENCES

1. Rossi RL, Cady B, Meissner WA, Wool MS, Sedgwick CE, Werber J. Nonfamilial medullary thyroid carcinoma. *Am J Surg* 1980;139:554–560.
2. Samaan NA, Schultz PN, Hickey RC. Medullary thyroid carcinoma: prognosis of familial versus sporadic disease and the role of radiotherapy. *J Clin Endocrinol Metab* 1988;67:801–808.
3. Schroder S, Bocker W, Baisch H, et al. Prognostic factors in medullary thyroid carcinomas. Survival in relation to age, sex, stage, histology, immunocytochemistry and DNA content. *Cancer* 1988;61:806–816.
4. Norton JA, Levin B, Jensen R. Cancer of the endocrine system. In: DeVita VT, Hellman S, Rosenberg SA, eds. *Cancer: Principles and practices of oncology*. New York: JB Lippincott Co; 1989;1333–1435.
5. Cance WG, Wells SA Jr. Multiple endocrine neoplasia type IIa. *Curr Probl Surg* 1985;22:1.
6. Tubiana M, Haddad E, Schlumberger M, Hill C, Rougier P, Sarrazin D. External radiotherapy in thyroid cancer. *Cancer* 1985;55:2062–2071.
7. Wells SA Jr, Dilley WG, Farndon JA, Leight GS, Baylin SB. Early diagnosis and treatment of medullary carcinoma. *Arch Intern Med* 1985;145:1248–1252.
8. Busnardo B, Girelli ME, Simioni N, Nacamulli D, Busetto E. Nonparallel patterns of calcitonin and carcinoembryonic antigen levels in the follow-up of medullary thyroid carcinoma. *Cancer* 1984;53:278–285.
9. Ishikawa N, Hamada S. Association of medullary carcinoma of the thyroid with carcinoembryonic antigen. *Br J Cancer* 1976;34:111–115.
10. Wells SA Jr, Haagensen DE Jr, Linehan WM, Farrell RE, Dilley WG. The detection of elevated plasma levels of carcinoembryonic antigen in patients with suspected or established medullary thyroid carcinoma. *Cancer* 1978;42:1498–1503.
11. Rougier PH, Calmettes C, Laplanche A, et al. The values of calcitonin and carcinoembryonic antigen in the treatment and management of nonfamilial medullary thyroid carcinoma. *Cancer* 1983;51:855–862.
12. Juweid M, Sharkey RM, Behr T, et al. Improved detection of medullary thyroid cancer with radiolabeled antibodies to carcinoembryonic antigen. *J Clin Oncol* 1996;14: 1209–1217.
13. Primus FJ, Newell KD, Blue A, Goldenberg DM. Immunological heterogeneity of carcinoembryonic antigen: Antigenic determinants on carcinoembryonic antigen distinguished by monoclonal antibodies. *Cancer Res* 1983;43:686–692.
14. Hansen HJ, Goldenberg DM, Newman ES, Grebenau R, Sharkey RM. Characterization of second-generation monoclonal antibodies against carcinoembryonic antigen. *Cancer* 1993;71:3478–3485.
15. Sharkey RM, Goldenberg DM, Murthy S, et al. Clinical evaluation of tumor targeting with a high-affinity, anticarcinoembryonic-antigen-specific, murine monoclonal antibody, MN-14. *Cancer* 1993;71:2082–2096.
16. Sharkey RM, Goldenberg DM, Goldenberg H, et al. Murine monoclonal antibodies against carcinoembryonic antigen: immunological, pharmacokinetic and targeting properties in humans. *Cancer Res* 1990;50:2823–2831.
17. Primus FJ, Kelley EA, Hansen HJ, Goldenberg DM. "Sandwich"-type immunoassay for carcinoembryonic antigen in patients receiving murine monoclonal antibodies for diagnosis and therapy. *Clin Chem* 1988;34(2):261–264.
18. Siegel JA, Pawlyk DA, Lee RE, et al. Tumor, red marrow and organ dosimetry for ^{131}I-labeled anti-carcinoembryonic antigen monoclonal antibody. *Cancer Res* 1990; 50:1039s–1042s.
19. Siegel JA, Goldenberg DM, Sharkey RM, et al. Tumor and organ dosimetry for ^{131}I-labeled LL2 (EPB2) monoclonal antibody in patients with B-cell lymphomas. *Antibod Immunoconj Radiopharm* 1991;4:649–654.
20. Loevinger R, Berman M. A revised scheme for calculating the absorbed dose from biologically distributed radionuclide. *MIRD pamphlet no. 1*, revised. New York: *Society of Nuclear Medicine*; 1976.
21. Bigler R, Zanzonico PB, Leonard R, et al. Bone marrow dosimetry for monoclonal antibody therapy. *Proceeding of the 4th International Radiopharmaceutical Dosimetry Symposium*, Oak Ridge, TN: 1985:535–544.
22. Cloutier RV, Watson EE, Rohrer RH, et al. Calculating the radiation dose to an organ. *J Nucl Med* 1973;14:53–55.
23. Peltier P, Curtet C, Chatal JF, et al. Radioimmunodetection of medullary thyroid cancer using a bispecific anti-CEA/anti-indium-DTPA antibody and an indium-111-labeled DTPA dimer. *J Nucl Med* 1993;34:1267–1273.
24. Vuillez JP, Peltier P, Caravel JP, Chetanneau A, Saccavini JC, Chatal JF. Immunoscintigraphy using ^{111}In-labeled F(ab')$_2$ fragments of anticarcinoembryonic antigen monoclonal antibody for detecting recurrences of medullary thyroid carcinoma. *J Clin Endocrinol Metab* 1992;74:157–163.
25. Edington HD, Watson CG, Levine G, et al. Radioimmunoimaging of metastatic medullary carcinoma of the thyroid gland using an indium-111-labeled monoclonal antibody to CEA. *Surgery* 1988;104:1004–1010.
26. Zanin DEA, van Dongen A, Hoefnagel CA, Bruning PF. Radioimmunoscintigraphy using iodine-131-anti-CEA monoclonal antibodies and thallium-201 scintigraphy in medullary thyroid carcinoma: a case report. *J Nucl Med* 1990;31:1854–1855.
27. Reiners CH, Eilles CH, Spiegel W, Becker W, Borner W. Immunoscintigraphy in medullary thyroid cancer using an ^{123}I or ^{111}In-labeled monoclonal anti-CEA antibody fragment. *Nuklearmedizin* 1986;25:227–231.
28. Behr T, Sharkey RM, Juweid M, et al. Influence of antibody protein on the dosimetry and diagnostic accuracy in radioimmunodetection (RAID) and therapy (RAIT) of CEA-expressing tumors [Abstract]. *J Nucl Med* 1995;36:226.
29. Murray JL, Rosenblum MG, Lamki L, et al. Clinical parameters related to optimal tumor localization of ^{111}In-labeled mouse antimelanoma monoclonal antibody ZME-018. *J Nucl Med* 1987;28:25–33.
30. Halpern SE, Haindl W, Beauregard J, et al. Scintigraphy with ^{111}In-labeled monoclonal antitumor antibodies: kinetics, biodistribution and tumor detection. *Radiology* 1988;168:529–536.
31. Patt YZ, Lamki LM, Haynie TP, et al. Improved tumor localization with increasing dose of ^{111}In-labeled anti-carcinoembryonic antigen monoclonal antibody ZCE-025 in metastatic colorectal cancer. *J Clin Oncol* 1988;6:1220–1230.